 DOI 10.1002/mnfr.201000381 *Mol. Nutr. Food Res.* 2011, *55*, 560–567

RESEARCH ARTICLE

Absorption and metabolism of the mycotoxin zearalenone and the growth promotor zeranol in Caco-2 cells *in vitro*

Erika Pfeiffer, Anne Kommer, Julia S. Dempe, Andreas A. Hildebrand and Manfred Metzler

Institute of Applied Biosciences, Karlsruhe Institute of Technology, Karlsruhe, Germany

Received: August 13, 2010
Revised: September 25, 2010
Accepted: October 12, 2010

Scope: Zearalenone (ZEN) and α-zearalanol (α-ZAL, zeranol) were studied in differentiated Caco-2 cells and in the Caco-2 Millicell® system *in vitro* to simulate their *in vivo* intestinal absorption and metabolism in humans.
Methods and results: In addition to metabolic reduction/oxidation, extensive conjugation with glucuronic acid and sulfate of the parent compounds and their phase I metabolites was observed. The positional isomers of the glucuronides and sulfates were unambiguously identified: Sulfonation occurred specifically at the 14-hydroxyl group, whereas glucuronidation was less specific and, in addition to the preferred 14-hydroxyl group, involved the 16- and 7-hydroxyl groups. Using the Caco-2 Millicell® system, an efficient transfer of the glucuronides and sulfates of ZEN and α-ZAL and their phase I metabolites into both the basolateral and the apical compartment was observed after apical administration. The apparent permeability coefficients (P_{app} values) of ZEN, α-ZAL and the ZEN metabolite α-zearalenol were determined, using an initial apical concentration of 20 μM and a permeation time of 1 h.
Conclusion: According to the P_{app} values, the three compounds are expected to be extensively and rapidly absorbed from the intestinal lumen *in vivo* and reach the portal blood both as aglycones and as glucuronide and sulfate conjugates in humans.

Keywords:
Caco-2 cells / Glucuronide / Sulfate / Zearalenone / Zeranol

1 Introduction

Zearalenone (ZEN, Fig. 1) is a macrocylic β-resorcylic acid lactone (RAL) produced by a variety of *Fusarium* fungal species, which are common in regions with temperate and warm climate. ZEN contaminates frequently corn and other cereal crops used for food and feed items. It causes reproductive problems in livestock, especially pigs, and possibly in humans due to its pronounced estrogenic activity [1–3]. More recently, ZEN has been disclosed as a micropollutant of drinking water inoculated with *Fusarium graminearum* [4], and of surface water in Switzerland and Poland [5, 6]. Shortly after the chemical structure of ZEN had been elucidated, it was observed that two of its reduction products, *i.e.* the α-stereoisomers of zearalenol (ZEL) and zearalanol (ZAL), are even more estrogenic than ZEN [3]. α-ZAL is also named zeranol or RalGro® and used as a hormonal growth promotor for cattle in the United States of America and Canada but not in Europe [2]. The α- and β-epimers of ZEL are major phase I metabolites of ZEN after ingestion in many mammalian species, and α-ZAL is likewise metabolized to zearalanone (ZAN) and β-ZAL (also called taleranol) in animals and humans [3]. The chemical structures of these closely related members of the 'ZEN family' are depicted in Fig. 1.

Correspondence: Professor Manfred Metzler, Institute of Applied Biosciences, Karlsruhe Institute of Technology (KIT), Adenauerring 20a, D-76131 Karlsruhe, Germany
E-mail: manfred.metzler@kit.edu
Fax: +49-721-6087255

Abbreviations: **HBSS,** Hanks' buffered salt solution; **HSD,** hydroxysteroid dehydrogenase; **PAPS,** 3′-phosphoadenosine-5′-phosphosulfate; **RAL,** β-resorcylic acid lactone; **ZAL,** zearalanol; **ZAN,** zearalanone; **ZEL,** zearalenol; **ZEN,** zearalenone

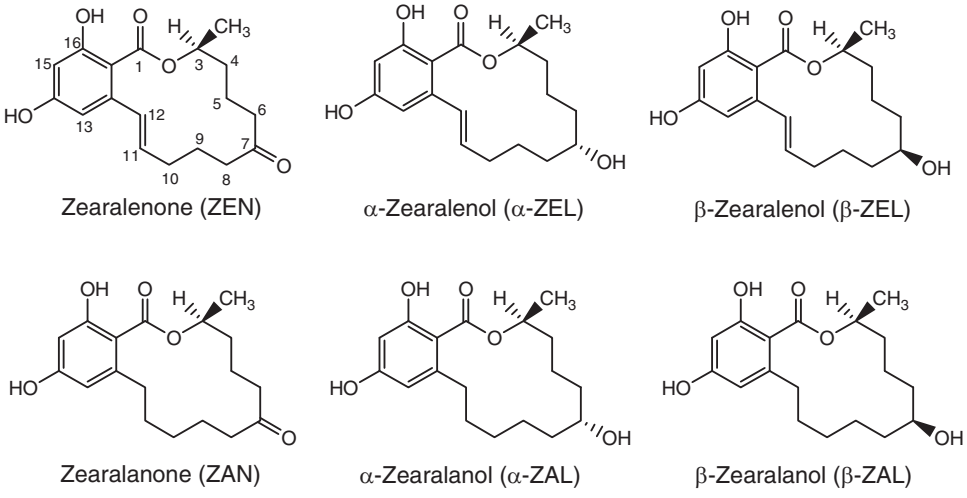

Figure 1. Chemical structures of ZEN and its reductive metabolites.

An important prerequisite for assessing the risk of ZEN and α-ZAL for human health is accurate data on the bioavailability after oral exposure. Studies in various animal species *in vivo* suggest that ZEN is efficiently absorbed from the gastrointestinal tract, but no data are available for humans [3]. Limited data exist for the disposition of α-ZAL in humans and several animal species, which also suggest good intestinal bioavailability [7].

A detailed knowledge of the fate of ZEN and α-ZAL in the human intestine is desirable, as the intestinal epithelium is the first barrier for absorption and site for metabolism of xenobiotic compounds after oral administration. To this end, the present study used cultured Caco-2 cells, which represent a widely accepted *in vitro* system for human intestinal absorption and metabolism [8–10]. Although derived from a human colon tumor, cultured Caco-2 cells feature many characteristics of intestinal epithelial cells, including the formation of a polarized monolayer with tight junctions and microvilli at the apical side, expression of transport proteins of the ABC superfamily, and activity of various enzymes for phase I and II metabolism [10]. The metabolism of ZEN has been studied in Caco-2 cells, and reduction of ZEN to α- and β-ZEL as well as glucuronide formation of the three RALs have been observed [11, 12]. However, the glucuronides have not been completely characterized, and sulfate conjugation has not been addressed.

In the present study, the exact structures of the glucuronides and sulfates generated in Caco-2 cells from ZEN, α-ZEL, and β-ZEL have been elucidated. Moreover, the phase I and II metabolism of the growth promotor α-ZAL and its metabolites ZAN and β-ZAL have been investigated in detail in this cell system. The basolateral and apical release of the parent RALs and their metabolites were determined after apical administration of ZEN and α-ZAL. Finally, the apparent permeability coefficients, which are believed to correlate well with intestinal drug absorption in humans *in vivo*, have been determined for ZEN, α-ZEL, and α-ZAL in Caco-2 cells *in vitro*.

2 Materials and methods

2.1 Chemicals and reagents

ZEN was purchased from Fermentek (Jerusalem, Israel). ZAN and the α- and β-stereoisomers of ZEL and ZAL were obtained from Sigma/Aldrich/Fluka (Taufkirchen, Germany). All compounds had a purity of >98% according to the manufacturers' certificates. ZEN-14-*O*-sulfate and ZEN-14-*O*-glucuronide were kindly provided by Dr. Franz Berthiller. 3′-Phosphoadenosine-5′-phosphosulfate (PAPS), β-glucuronidase type B-1 from bovine liver, sulfatase from *Aerobacter aerogenes*, and all other chemicals and reagents were also obtained from Sigma/Aldrich/Fluka.

2.2 Formation of sulfates in rat liver cytosol

In order to generate standards for the identification of the sulfate conjugates, the six RALs were separately incubated with rat liver cytosol prepared as the 100 000 × *g* supernatant of a liver homogenate from untreated male Wistar rats. Incubation mixtures consisted of a total volume of 200 µL of 0.1 M potassium phosphate buffer (pH 7.4) containing 50 µM RAL dissolved in DMSO, 10 mM $MgCl_2$, 0.4 mM PAPS, and 200 µg cytosolic protein. The DMSO concentration did not exceed 1% in the final incubations. A mixture containing all constituents except PAPS was preincubated for 5 min at 37°C, PAPS dissolved in phosphate buffer was added, and the incubation continued for 30 min with gentle shaking. Subsequently, the mixture was centrifuged for 5 min at 2000 × *g*, and the supernatant directly analyzed by LC-DAD-MS. The spectral and chromatographic information obtained from the sulfates thus generated was used to identify the sulfates formed in Caco-2 cells.

Authentic ZEN-14-*O*-sulfate was dissolved in methanol and reduced with sodium borohydride to yield a mixture of α-ZEL-14-*O*-sulfate and β-ZEL-14-*O*-sulfate. When a

solution of ZEN-14-*O*-sulfate in methanol was stirred under hydrogen gas for 10 h in the presence of 10% Pd on activated carbon as a catalyst, a mixture of ZAN-14-*O*-sulfate and the α- and β-isomers of ZAL-14-*O*-sulfate was formed.

2.3 Caco-2 cell culture and subculture

Caco-2 cells were from Deutsche Sammlung von Mikroorganismen und Zellkulturen GmbH (Braunschweig, Germany, DSMZ No. ACC169). Cells were cultured at 37°C and 5% CO_2 in dishes with 15-cm diameter containing 20 mL medium and initially 0.4×10^6 cells. The culture medium consisted of Dulbecco's modified Eagle medium (DMEM/F12, purchased from Sigma) with 10% fetal calf serum, 100 U/mL penicillin, and 100 μg/mL streptomycin, and was replaced every 2 days. After 7 days, the medium was removed and the attached cells were washed twice with 10 mL PBS each, followed by treatment with 2.5 mL of a 0.625% aqueous trypsin solution for 40 s. After removal of the trypsin, cells were incubated at 37°C for 5 min and suspended subsequently in 10 mL medium. Cell number was determined in a 1:10 dilution using a Neubauer chamber, and the volume containing 0.4×10^6 cells was transferred to a new dish.

2.4 Metabolism of the RALs in Caco-2 cells

For studying the metabolism of the six RALs in differentiated Caco-2 cells, 10^6 cells *per* well were seeded into six-well dishes (without insert) and grown for 21 days with renewal of the medium every 2 days. On day 21, the medium was removed and the cells were washed twice with Hanks' buffered salt solution (HBSS), containing 8 g/L NaCl, 0.40 g/L KCl, 0.14 g/L $CaCl_2$, 0.03 g/L $MgCl_2$, 0.05 g/L $MgSO_4$, 0.50 g/L NaH_2PO_4, 0.05 g/L Na_2HPO_4, 0.06 g/L K_2HPO_4, 1 g/L glucose, and adjusted to pH 7.4 with 1 N aqueous HCl. Subsequently, HBSS containing the substance at 40 μM with 1% DMSO was added. After a 3-h incubation, the total fluid of each well was removed for analysis LC-DAD-MS. The attached cells of each well were washed twice with 2 mL PBS each, scraped off the support with a plastic spatula, suspended in 1 mL HBSS, and transferred into a 2-mL centrifuge vial. The pellet obtained after centrifugation at $1000 \times g$ for 5 min was resuspended in 0.2 mL HBSS and lysed at −80°C for 24 h. After ultrasonic treatment, 20 μL of a 5 mM solution of 4,4′-isopropylidenbis(2,6-dimethylphenol) in DMSO was added to facilitate the quantification of the mycotoxin metabolites as described recently [13]. For the analysis of unconjugated mycotoxins, 100 μL of the lysate was diluted with the same volume of 0.1 M potassium phosphate buffer (pH 7.4) and extracted three times with 0.5 mL each of ethyl acetate. For the analysis of conjugates, other aliquots of the lysate were diluted with 0.1 M potassium phosphate buffer (pH 7.1) and incubated for 2 h at 37°C with 250 U of β-glucuronidase from bovine liver or 0.2 U of sulfatase from *A. aerogenes*, containing a maximum of 0.07 U of β-glucuronidase. After extraction with ethyl acetate, all extracts were evaporated to dryness under a stream of nitrogen and the residues dissolved in 100 μL methanol and analyzed by LC-DAD-MS without further purification.

2.5 Caco-2 Millicell® system and *in vitro* absorption of ZEN and α-ZAL

Each insert (apical compartment) of the 24-well Millicell® plates (Millipore, Billerica, MA, USA) was filled with 0.4 mL medium containing 6×10^4 cells, and each well (basolateral compartment) received 0.8 mL medium alone. Cells were grown into a differentiated monolayer for 21 days, with renewal of the medium in both compartments every other day. Then the medium was removed and the apical and the basolateral compartments were washed twice with HBSS. Subsequently, HBSS containing a defined concentration of ZEN or α-ZAL was filled into the apical compartment, whereas the basolateral compartment contained only HBSS. Ten, 20, 30, and 40 μM ZEN or α-ZAL were incubated for 3 h, and 20 μM ZEN or α-ZAL for 1, 2, 4, and 6 h. Both compartments were analyzed by LC-DAD-MS.

In order to ensure an intact monolayer of the Caco-2 cells, both compartments of each well were washed once with HBSS after each experiment, and 0.4 mL of HBSS containing 100 μg lucifer yellow *per* mL was filled into the apical well, whereas the basolateral compartment contained dye-free HBSS. After 1 h at 37°C, 200 μL of the basolateral HBSS was analyzed for lucifer yellow fluorimetrically (excitation at 485 nm and emission at 535 nm). Only cell layers with $<1\%$ transfer of the dye from the apical to the basolateral side were considered intact [14].

2.6 LC-DAD-MS analysis

A LXQ Linear Ion Trap MSn system (Thermo Fisher Scientific, Waltham, MA, USA) equipped with a Finnigan Surveyor Autosampler Plus and a Finnigan Surveyer PDA Plus Detector was used. This allowed online detection of UV absorption and mass spectrometry. Separation was carried out on a 250 mm × 4.6 mm id, 5 μm, reversed phase Luna C18 column (Phenomenex, Torrance, CA, USA) protected by a 3 mm × 4.0 mm id SecurityGuard C18 (ODS) column (Phenomenex). Solvent A was deionized water containing 5 mM ammonium acetate, and solvent B was ACN with 0.1% formic acid. Elution started with a linear increase from 30% B to 100% B within 30 min. After 5 min at 100% B, the initial 30% B were reached in 1 min and kept for 5 min before the next sample was injected. The flow rate was 0.5 mL/min, and the detection wavelengths were 280 and

260 nm. The mass spectrometer was operated in the negative ESI mode. Nitrogen was used as the sheath gas, auxiliary gas, and sweep gas with flow rates of 30.0, 15.0, and 0.02 L/min, respectively. Spray voltage was 4.47 kV, spray current 3.15 μA, capillary voltage −45.10 V, capillary temperature 350°C, and tube lens voltage 125.58 V. Full scan mass spectra were recorded from m/z 100 to 600 in order to confirm the identity of the compounds through their [M–H] ions.

Quantitation of the RALs and their conjugates by DAD was carried out at 280 nm for the RALs with the aliphatic double bond and 260 nm for those without double bond. The absorbance of ZEN did not differ significantly from that of ZEN-14-*O*-glucuronide and ZEN-14-*O*-sulfate, which were considered as standards. Therefore, it was assumed that the conjugates of the other RALs had the same absorbance as their aglycones. The peak area corresponding to 0.5–1 pmol was the limit of quantitation, with a signal-to-noise ratio of 10:1.

2.7 Calculation of P_{app}

P_{app} values were calculated according to Artursson and Karlsson [8] using the formula

$$P_{app}(\mathrm{cm\,s^{-1}}) = (V_{api}/A \bullet t)(C_{baso}/C_{api}) \quad (1)$$

where V_{api} is the volume of the apical compartment (0.4 mL), A the surface area of the monolayer (0.7 cm^2), t the time (s), C_{baso} the concentration (μM) of the compound in the basolateral compartment (either parent compound or the sum of the parent compound and metabolites), and C_{api} the initial concentration (μM) of mycotoxin in the apical compartment.

3 Results and discussion

3.1 Characterization of the glucuronides and sulfates of the six RALs

Because two or three different monoglucuronides and monosulfates can be formed from each RAL depending on the number of hydroxyl groups, reference compounds were needed for the unambiguous identification of the RAL conjugates formed in Caco-2 cells. The monoglucuronides (Table 1) were enzymatically prepared and identified as described earlier [15]. ZEN-14-*O*-sulfate was isolated from *F. graminearum*-inoculated rice and characterized in the laboratory of Franz Berthiller [16]. Its reduction with sodium borohydride gave rise to a mixture of α- and β-ZEL-14-*O*-sulfate, which had markedly different retention times in HPLC. In analogy with the respective glucuronides, it was assumed that the β-isomer eluted earlier than the α-isomer from a reversed phase column. Catalytic hydrogenation of ZEN-14-*O*-sulfate yielded mostly ZAN-14-*O*-sulfate, together with small amounts of α- and β-ZAL-14-*O*-sulfate. A complete set of the sulfates of the six RALs (Table 1) was obtained by incubating the aglycones with rat liver cytosol in the presence of PAPS, followed by the analysis of the

Table 1. Characterization of the monoglucuronides (G) and monosulfates (S) of the six RALs

RAL	MS^2 of [M–H][a]			Glucuronide	RT	MS^2 of [M–H]			Sulfate	RT	MS^2 of [M–H]		
	RT	[M–H][b]	[M–H–CO_2]			[M–H]	[M–H–CO_2]	[M–H–G]			[M–H]	[M–H–CO_2]	[M–H–S]
ZEN	21.8	317	273 (100)	14-*O*-G	11.3	493	n.d.[c]	317 (100)	14-*O*-S	16.7	397	n.d.	317 (100)
				16-*O*-G	8.1	493	449 (45)	317 (100)	16-*O*-S	12.8	397	n.d.	317 (100)
α-ZEL	18.1	319	275 (100)	7-*O*-G	10.0	495	451 (100)	319 (4)	7-*O*-S	15.0	399	355 (100)	319 (65)
				14-*O*-G	8.2	495	n.d.	319 (100)	14-*O*-S	14.4	399	n.d.	319 (100)
				16-*O*-G	5.2	495	451 (11)	319 (100)	16-*O*-S	9.6	399	n.d.	319 (100)
β-ZEL	15.7	319	275 (100)	7-*O*-G	8.3	495	451 (100)	319 (7)	7-*O*-S	12.5	399	355 (100)	319 (40)
				14-*O*-G	6.4	495	n.d.	319 (100)	14-*O*-S	11.2	399	n.d.	319 (100)
				16-*O*-G	5.1	495	451 (11)	319 (100)	16-*O*-S	9.2	399	n.d.	319 (100)
ZAN	21.7	319	275 (100)	14-*O*-G	11.2	495	n.d.	319 (100)	14-*O*-S	16.8	399	n.d.	319 (100)
				16-*O*-G	8.0	495	451 (8)	319 (100)	16-*O*-S	12.8	399	n.d.	319 (100)
α-ZAL	17.9	321	277 (100)	7-*O*-G	10.6	497	453 (100)	321 (5)	7-*O*-S	13.3	401	357 (100)	321 (70)
				14-*O*-G	8.3	497	n.d.	321 (100)	14-*O*-S	12.4	401	n.d.	321 (100)
				16-*O*-G	7.3	497	453 (20)	321 (100)	16-*O*-S	11.1	401	n.d.	321 (100)
β-ZAL	15.0	321	277 (100)	7-*O*-G	8.8	497	453 (100)	321 (4)	7-*O*-S	12.0	401	357 (100)	321 (45)
				14-*O*-G	7.1	497	n.d.	321 (100)	14-*O*-S	11.2	401	n.d.	321 (100)
				16-*O*-G	6.3	497	453 (7)	321 (100)	16-*O*-S	9.4	401	n.d.	321 (100)

RT, retention time in LC-MS.
a) m/z.
b) m/z (relative intensity).
c) n.d., not detected (<3% relative intensity).

incubation mixtures using LC-DAD-MS. With each RAL, one predominant product was observed, which had a [M–H] ion corresponding to a monosulfate in the negative ESI mass spectrum (Table 1). The major sulfate of each RAL cochromatographed with the synthetic 14-*O*-sulfates and also had an identical MS^2 spectrum of the [M–H] ion. In addition to the major sulfate, small amounts of another monosulfate were formed from ZEN and ZAN, which must represent the respective 16-*O*-sulfates. With the epimers of ZEL and ZAL, two minor monosulfates were formed together with the major 14-*O*-sulfate and assumed to represent the 7-*O*-sulfates and 16-*O*-sulfates. The structure assignment was based on the comparison of the HPLC retention times and MS^2 spectra of the [M–H] ions with those of the glucuronides (Table 1). The positional isomer with the lowest retention time on the reversed phase column was always the 16-*O*-conjugate, followed by the 14-*O*-conjugate and the 7-*O*-conjugate. The lower polarity of the 7- and 14-*O*-conjugate as compared with the 16-*O*-conjugate is probably due to the strong hydrogen bonding of the free 16-hydroxyl group with the neighboring keto group at C-1. In the MS^2 spectra, a significant difference in fragmentation of the [M–H] ion was observed between the positional isomers carrying the sulfate group at the aromatic or aliphatic ring (Table 1). Whereas the only fragment ions observable in the MS^2 spectra of the 14- and 16-*O*-conjugates were the ions resulting from the release of the sulfate group, 7-*O*-conjugates preferred fragmentation at the lactone group with the release of carbon dioxide. The same tendency was noted for the positional isomers of the RAL glucuronides (Table 1), as has been already noted before [15, 17].

3.2 Metabolism of the RALs in Caco-2 cells

Differentiated Caco-2 cells grown in a normal cell culture dish without insert were incubated with 40 μM (80 nmol total amount) of each of the six RALs for 3 h, and the incubation buffer and the lysate of the Caco-2 cells were then analyzed using LC-DAD-MS. As typical examples, the LC profiles of the incubation media of ZEN and α-ZAL are depicted in Fig. 2.

In the incubation medium of ZEN, both the reductive metabolites α-ZEL and β-ZEL and several glucuronides and sulfates were identified by cochromatography with the reference compounds and by mass spectrometry. The major conjugates were the 14-*O*-glucuronides and 14-*O*-sulfates of ZEN and the ZEL epimers. Notably, small amounts of 7-*O*- and 16-*O*-glucuronides but not sulfates were generated in Caco-2 cells. A similar metabolism was observed for α-ZAL, yielding ZAN as the product of dehydrogenation at C-7 as well as 14-*O*-glucuronides and 14-*O*-sulfates as the major and 7-*O*- and 16-*O*-glucuronides as the minor conjugates (Fig. 2 and Table 2). The reduction/oxidation at C-7 is assumed to be catalyzed by 3α- and 3β-hydroxysteroid dehydrogenase (HSD) and leads to a mixture of the 7-keto

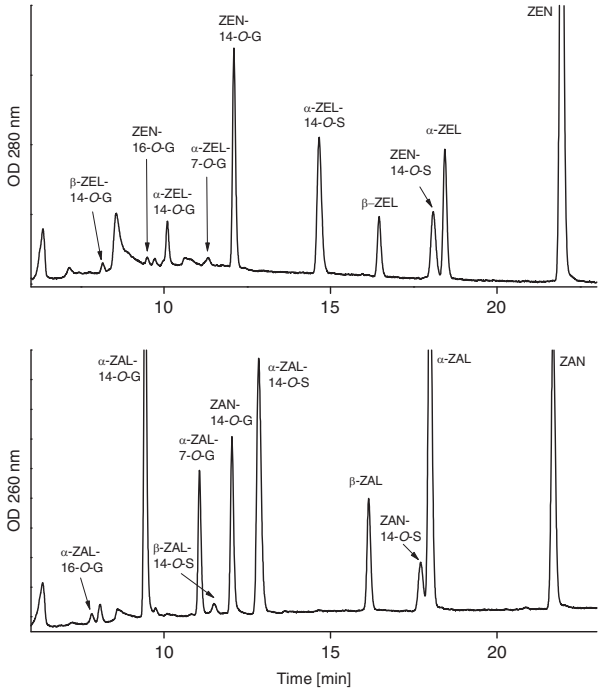

Figure 2. LC profile of the culture media of the 3-h incubation of Caco-2 cells with ZEN (top) and α-ZAL (bottom).

form and the two 7-hydroxy epimers [18]. The reduction of ZEN to α- and β-ZEL and the expression of 3α- and 3β-HSD have recently been demonstrated in Caco-2 cells [12].

The pattern of metabolites of ZEN and α-ZAL observed in the culture medium of Caco-2 cells was very similar for the other four RALs, although some differences were noted regarding the extent and the pattern of HSD-mediated metabolism (Table 2): RALs with an olefinic double bond appeared to prefer the 7-keto form, as the extent of conversion of ZEN by HSD was only 26% and the keto forms represented 94 and 81% of the conversion products of α-ZEL and β-ZEL, respectively. In contrast, RALs without an olefinic double bond preferred the 7α-hydroxy form, indicated by the 53% conversion of ZAN to a mixture of α- and β-ZAL, of which 61% was α-ZAL. Also, the conversion products of β-ZAL comprised 54% α-ZAL but only 46% ZAN (Table 2).

The extent of conjugation appeared to depend primarily on the status of the C-7 group: the α-epimers of ZEL and ZAL exhibited about 50% conjugation, the ketones ZEN and ZAN about 25%, and the β-epimers of ZEL and ZAL about 15% (Table 2). With most RALs, glucuronidation exceeded sulfonation, and only α-ZEL gave rise to equal amounts of both conjugates.

Differences were noted with respect to the distribution of the RALs and their metabolites between culture medium and the lysate of Caco-2 cells. The highest intracellular amount (about 30%) was obtained with ZEN and α-ZEL, and the lowest (5%) with β-ZAL, whereas β-ZEL, ZAN, and α-ZAL were intermediate with about 15% (Fig. 3). LC-DAD-

Table 2. Profile of metabolites in the culture medium of Caco-2 cells after 3-h incubation with 40 μM of each of six RALs (% of recovered material)

Metabolite fraction	ZEN	α-ZEL	ß-ZEL	ZAN	α-ZAL	β-ZAL
Sum of unconjugated and conjugated parent RAL	73.8±2.9[a)]	61.7±1.8	61.3±2.6	46.9±3.9	61.3±3.0	70.4±1.9
Unconjugated parent RAL	57.5	30.9	53.3	33.7	31.3	58.4
Glucuronides of parent RAL	11.1	14.8	4.9	9.4	19.0	7.0
16-/14-/7-*O*-conjugate[b)]	3/97/n.a.[c)]	0/89/11	17/67/16	0/100/n.a.	4/70/26	12/74/14
Sulfates of parent RAL (14-*O*-conjugate)	5.2	16.0	3.1	3.8	11.0	5.0
Sum of phase I metabolites at C-7[d)]	26.2	38.3	38.7	53.1	38.7	29.6
α-hydroxy/β-hydroxy/keto form	22/4/n.a.	n.a./2/36	7/n.a./32	32/21/n.a.	n.a./11/28	16/n.a./14

a) Mean value±standard deviation of three independent incubations.
b) % of total conjugates.
c) n.a., not applicable.
d) only unconjugated material; the ratio of unconjugated to conjugated phase I metabolites was about the same as for the parent RALs, and the small amounts of conjugated phase I metabolites were ignored.

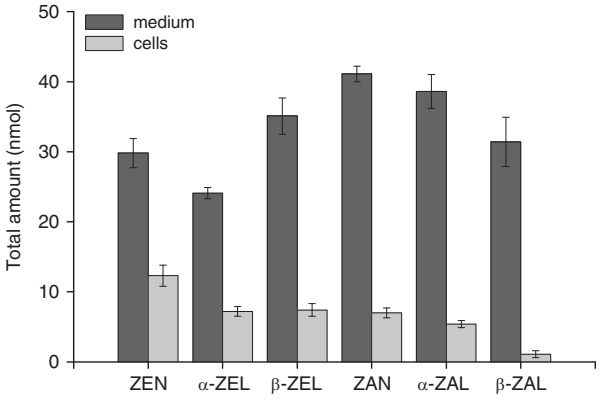

Figure 3. Distribution of various RALs and their metabolites between incubation media and Caco-2 cells after 3-h incubation. Data represent mean and standard deviation of recovered material in three independent incubations of 80 nmol RAL.

MS analysis of the intracellular material showed that 90% was unconjugated and consisted predominantly (about 80%) of the keto form with each of the six RALs (data not shown). These findings imply that the 7-hydroxy forms are more readily conjugated than the 7-keto forms, and conjugates are rapidly excreted from the cells into the culture medium.

In summary, Caco-2 cells are capable of reduction/oxidation of the functional group at C-7 of RALs, and of glucuronidation and sulfonation, preferentially at the 14-hydroxyl group. Both types of conjugates are eliminated from the cells.

3.3 Absorption and metabolism of ZEN and α-ZAL in the Caco-2 Millicell® system

Monolayers of differentiated Caco-2 cells were used to determine the *in vitro* absorption of ZEN and α-ZAL. Cells were first exposed to 10, 20, 30, and 40 μM ZEN or α-ZAL for 3 h and the phase I metabolites (conversion at C-7) and conjugates determined in both compartments (Fig. 4). Whereas the amount of phase I metabolites increased with increasing RAL concentration, the amount of glucuronides and sulfates reached a plateau at 20 μM, suggesting saturation of the conjugating enzymes. The pattern of C-7 conversion products and conjugates was consistent with the results of the previous metabolism study listed in Table 2.

The results of the kinetic study are depicted in Fig. 5. Whereas the concentration of unconjugated ZEN appeared to decrease with first-order kinetics at the apical side, its basolateral increase reached a plateau after approximately 2 h. ZEN conversion products and sulfates exhibited a slow basolateral and apical increase. The dominant metabolites were ZEN glucuronides, which accumulated at about the same rate in the basolateral and apical compartment (Fig. 5, left chart).

With α-ZAL (Fig. 5, right chart), a higher rate of conversion at C-7 was noted in comparison with ZEN. As with ZEN, glucuronidation was preferred to sulfonation with α-ZAL, but unlike ZEN, both conjugates of α-ZAL were preferentially excreted into the basolateral compartment. Interestingly, the 7-*O*-glucuronide of α-ZAL, which represents 25% of the glucuronides (Table 2) was eliminated exclusively at the basolateral side (data not shown).

3.4 Apparent permeability coefficient P_{app} of ZEN, α-ZEL, and α-ZAL

The transition of a compound from the apical to the basolateral compartment in the Caco-2 Millicell® system is expressed commonly by its P_{app} value, which correlates well with the absorption of xenobiotic compounds by humans *in vivo* [8–10]. The P_{app} values obtained with a concentration of 20 μM in the apical compartment and an incubation time of 1 h were $10.4 \pm 4.7 \times 10^{-6}$ cm/s for parent ZEN, $5.4 \pm 0.5 \times 10^{-6}$ cm/s for parent α-ZEL, and $15.0 \pm 2.5 \times 10^{-6}$ cm/s for parent α-ZAL. For the sum of the parent RAL and its metabolites, P_{app} values were

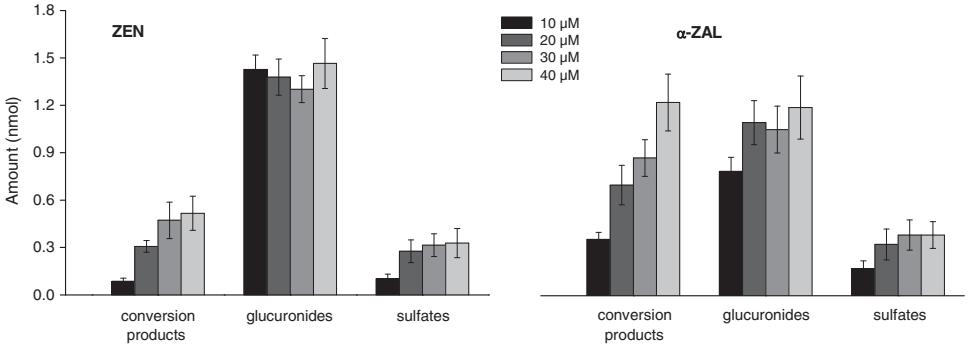

Figure 4. The sum of phase I metabolites (conversion products at C-7) and conjugates in the apical and basolateral compartments of Millicell® plates containing Caco-2 cell monolayers and various concentrations of ZEN (left chart) and α-ZAL (right chart) after 3-h incubation. The concentration of 10 µM corresponds to a total amount of 4 nmol RAL in the incubation. Data are mean ± standard deviation of three independent incubations.

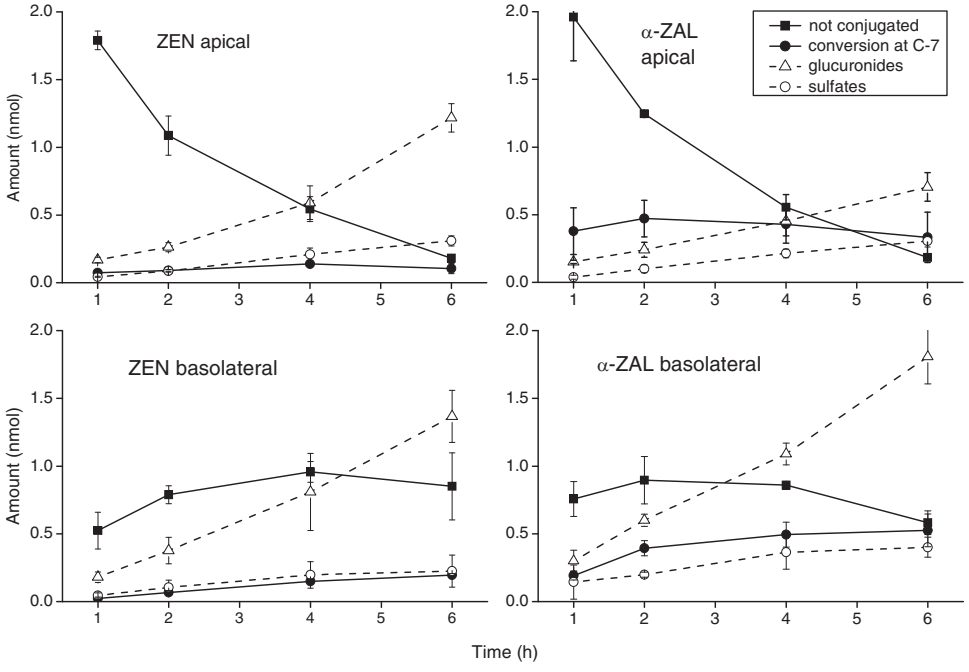

Figure 5. Time-course experiment of the amounts of parent RAL and its phase I and II metabolites in the apical and basolateral compartment of Millicell® plates containing Caco-2 cell monolayers and an initial concentration of 20 µM ZEN (left chart) and α-ZAL (right chart), corresponding to 8 nmol. Data are mean ± standard deviation of three independent incubations.

$15.4 \pm 5.2 \times 10^{-6}$ cm/s for ZEN, $16.2 \pm 1.6 \times 10^{-6}$ cm/s for α-ZEL, and $26.1 \pm 2.3 \times 10^{-6}$ cm/s for α-ZAL.

According to the correlation of P_{app} values determined in Caco-2 cells *in vitro* with human absorption *in vivo*, P_{app} values $> 10 \times 10^{-6}$ cm/s predict high (80–100%) absorption, whereas P_{app} values between 1 and 10×10^{-6} cm/s predict moderate (20–80%), and $P_{app} < 1 \times 10^{-6}$ cm/s low (0–20%) absorption [9, 10]. Thus, ZEN and α-ZAL must be expected to be efficiently absorbed from the human gastrointestinal tract and to reach the portal blood both as aglycones and as glucuronide and sulfate conjugates. This conclusion is consistent with the published data on the oral bioavailability of ZEN and α-ZAL. Although no *in vivo* data on the gastrointestinal absorption of ZEN in humans are available, studies in various animal species suggest that orally administered ZEN is absorbed fairly rapidly and to a high extent in rat, rabbit, pig, and cow [1] and in immature pigs [19]. For α-ZAL, *in vivo* studies on the absorption and disposition have been conducted in the rat, rabbit, dog, Rhesus monkey, and man with ^{3}H-labeled compound [7]. α-[^{3}H]ZAL was found to be efficiently absorbed in all species.

4 Concluding remarks

Our study has, for the first time, elucidated the exact chemical structures of all conceivable monosulfates of ZEN and α-ZAL and their HSD-mediated metabolites α- and

β-ZEL, ZAN, and β-ZAL, thus complimenting recent reports on the monoglucuronides of the six RALs [15, 17]. Using this information, the glucuronides and the sulfates generated from the six RALs in cultured Caco-2 cells have been determined. All RALs were found to preferentially form glucuronides at the 14-hydroxyl group, but small amounts of 16-*O*-glucuronides and, with the epimers of ZEL and ZAL, 7-*O*-glucuronides were also observed. In contrast, sulfonation of the six RALs occurred exclusively at the 14-hydroxyl group. The ratio of glucuronide-to-sulfate formation ranged from about 2.1 to 0.9, depending on the individual RAL. After apical administration of ZEN, large amounts of glucuronides and smaller amounts of sulfates of ZEN and its reductive metabolites α-ZEL and β-ZEL were released almost equally well into the basolateral and apical compartments. A similar disposition in Caco-2 cells was observed for α-ZAL, except that the basolateral release was two- to threefold higher than the apical excretion. Thus, the parent ZEN, α-ZAL, and the HSD-mediated metabolites and conjugates must be assumed to reach the portal blood after oral delivery, with α-ZAL being somewhat better absorbed than ZEN. Finally, the apparent permeability coefficients calculated for ZEN, α-ZEL, and α-ZAL suggest high intestinal *in vivo* bioavailability for all three RALs in humans.

This study was supported by the Deutsche Forschungsgemeinschaft (Grant ME 574/32-1) and KIT (Research Program 'Mycotoxins' as part of the Research Initiative 'Food and Health'). The authors thank Dr. Franz Berthiller, University of Natural Resources and Applied Life Sciences, Vienna, Austria, for providing ZEN-14-O-sulfate.

The authors have declared no conflict of interest.

5 References

[1] Kuiper-Goodman, T., Scott, P. M., Watanabe, H., Risk assessment of the mycotoxin zearalenone. *Regul. Toxicol. Pharmacol.* 1987, *7*, 253–306.

[2] Zinedine, A., Soriano, J. M., Molto, J. C., Manes, J., Review on the toxicity, occurrence, metabolism, detoxification, regulations and intake of zearalenone: an oestrogenic mycotoxin. *Food Chem. Toxicol.* 2007, *45*, 1–18.

[3] Metzler, M., Pfeiffer, E., Hildebrand, A. A., Zearalenone and its metabolites as endocrine disrupting chemicals (EDC). *World Mycotoxin J.* 2010, *3*, 385–401.

[4] Paterson, R. R. M., Zearalenone production and growth in drinking water inoculated with *Fusarium graminearum*. *Mycol. Progress* 2007, *6*, 109–113.

[5] Buchell, T. D., Wettstein, F. E., Hartmann, N., Erbs, M. *et al.*, *Fusarium* mycotoxins: overlooked aquatic micropollutants? *J. Agric. Food Chem.* 2008, *56*, 1029–1034.

[6] Gromadzka, K., Waskiewicz, A., Golinski, P., Swietlik, J., Occurrence of estrogenic mycotoxin – zearalenone in aqueous environmental samples with various NOM content. *Water Res.* 2009, *43*, 1051–1059.

[7] Migdalof, B. H., Dugger, H. A., Heider, J. G., Coombs, R. A. *et al.*, Biotransformation of zeranol: disposition and metabolism in the female rat, rabbit, dog, monkey and man. *Xenobiotica* 1983, *13*, 209–221.

[8] Artursson, P., Karlsson, J., Correlation between oral drug absorption in humans and apparent drug permeability coefficients in human intestinal epithelial (Caco-2) cells. *Biochem. Biophys. Res. Commun.* 1991, *175*, 880–885.

[9] Yee, S., *In vitro* permeability across Caco-2 cells (colonic) can predict *in vivo* (small intestinal) absorption in man – fact or myth. *Pharm. Res.* 1997, *14*, 763–766.

[10] Press, B., Di Grandi, D., Permeability for intestinal absorption: Caco-2 assay and related issues. *Curr. Drug Metab.* 2008, *9*, 893–900.

[11] Schaut, A., De Saeger, S., Sergent, T., Schneider, Y. J. *et al.*, Study of the gastrointestinal biotransformation of zearalenone in a Caco-2 cell culture system with liquid chromatographic methods. *J. Appl. Toxicol.* 2008, *28*, 966–973.

[12] Videmann, B., Mazallon, M., Tep, J., Lecoeur, S., Metabolism and transfer of the mycotoxin zearalenone in human intestinal Caco-2 cells. *Food Chem. Toxicol.* 2008, *46*, 3279–3286.

[13] Pfeiffer, E., Herrmann, C., Altemöller, M., Podlech, J. *et al.*, Oxidative *in vitro* metabolism of the *Alternaria* toxins altenuene and isoaltenuene. *Mol. Nutr. Food Res.* 2009, *53*, 452–459.

[14] Gres, M. C., Julian, B., Bourrie, M., Meunier, V. *et al.*, Correlation between oral drug absorption in humans, and apparent drug permeability in TC-7 cells, a human epithelial intestinal cell line: comparison with the parental Caco-2 cell line. *Pharm. Res.* 1998, *15*, 726–733.

[15] Pfeiffer, E., Hildebrand, A., Mikula, H., Metzler, M., Glucuronidation of zearalenone, zeranol and four metabolites *in vitro*: formation of glucuronides by various microsomes and human UDP-glucuronosyltransferase isoforms. *Mol. Nutr. Food Res.* 2010, *54*, 1468–1476.

[16] Berthiller, F., Werner, U., Sulyok, M., Krska, R. *et al.*, Liquid chromatography coupled to tandem mass spectrometry (LC-MS/MS) determination of phase II metabolites of the mycotoxin zearalenone in the model plant *Arabidopsis thaliana*. *Food Addit. Contam.* 2006, *23*, 1194–1200.

[17] Stevenson, D. E., Hansen, R. P., Loader, J. I., Jensen, D. J. *et al.*, Preparative enzymatic synthesis of glucuronides of zearalenone and five of its metabolites. *J. Agric. Food Chem.* 2008, *56*, 4032–4038.

[18] Malekinejad, H., Maas-Bakker, R. F., Fink-Gremmels, J., Bioactivation of zearalenone by porcine hepatic biotransformation. *Vet. Res.* 2005, *36*, 799–810.

[19] Biehl, M. L., Prelusky, D. B., Koritz, G. D., Hartin, K. E. *et al.*, Biliary excretion and enterohepatic cycling of zearalenone in immature pigs. *Toxicol. Appl. Pharmacol.* 1993, *121*, 152–159.

